Int. J. Electrochem. Sci., 13 **(2018)** 9200 – 9213, doi: 10.20964/2018.09.09

International Journal of ELECTROCHEMICAL SCIENCE
www.electrochemsci.org

Novel One Pot Synthesis of Alkaline-reduced Iron Oxide/graphene Nanocomposites for Amperometric Non-enzymatic Glucose Sensor

Suyanta[1,*], *Siti Nur Akmar Mohd Yazid*[2], *Illyas Md Isa*[2,*], *Norhayati Hashim*[2], *Mohamad Syahrizal Ahmad*[2]

[1] Deparment of Chemistry Education, Faculty of Mathematics and Natural Science, Yogyakarta State University, Yogyakarta, Indonesia
[2] Department of Chemistry, Faculty of Science and Mathematics, Universiti Pendidikan Sultan Idris, 35900 Tanjung Malim, Perak, Malaysia.
[*]E-mail: suyanta@uny.ac.id ; illyas@fsmt.upsi.edu.my

Received: 1 January 2018 / *Accepted:* 30 May 2018 / *Published:* 5 August 2018

Recently, Fe_3O_4 nanostructures are studied extensively for the use of enzymatic glucose sensor applications. However, reports on the non-enzymatic sensing performance of Fe_3O_4 for direct oxidation of glucose are rare. Therefore, in this work, a novel glassy carbon electrode modified with iron oxide/graphene nanocomposites (Fe_3O_4/graphene/GCE) was used for the non-enzymatic amperometric determination of glucose. The Fe_3O_4/graphene nanocomposite was first synthesised in alkaline aqueous solution through a simple chemical reduction process. The modified electrode was then studied for a non-enzymatic glucose sensing application in 0.1 M KNO_3 supporting electrolyte (pH = 3.0). Under optimized conditions, the low detection limit of 0.18 µM with a linear range from 50 µM to 4.00 mM as well as good sensitivity (959.00 µA mM^{-1} cm^2), stability and reproducibility have been obtained using the Fe_3O_4/graphene/GCE, thus, leading to a promising candidate for non-enzymatic glucose detection. The sensor was employed for the testing of glucose concentration in real blood samples.

Keywords: Iron oxide nanoparticles, non-enzymatic glucose sensor, graphene, electrochemical sensor

1. INTRODUCTION

Diabetes mellitus has turn out to be one of the pandemic issues worldwide. The number of people who are diagnosed diabetes has increased thus troubling most developed societies. This problem has encouraged scientists to put great effort in the development of sensitive and selective glucose sensor in order to identify the human health conditions. Electrochemical sensors are the most

suitable owing to their simplicity, low cost and high performance [1]. Conventional electrochemical sensors usually require an immobilization of catalytic enzyme, such as glucose oxidase to perform glucose sensing. This enzyme is expensive, thus require a high cost to build the sensor. The nature of enzymes also affected the instability at the surface of electrode as they are easily interrupted by temperature, interferences, and humidity [2].

To overcome the limitations, great efforts have been made using the non-enzymatic glucose sensors to detect the glucose. Most glucose sensors reported to date have used electrochemical reactions involving metal oxide/graphene. Sensitivity and selectivity of the modified sensors had been reported to enhance the oxidation of glucose at electrode surface due to the combination of extraordinary properties of graphene and metal oxide nanoparticles. These sensors have presented great selectivity, good stability, resistance to thermal effects with low cost and a facile preparation method [3].

There have been some reports of electrochemical glucose sensors based on nanostructured Fe_3O_4. This metal oxide is non-toxic, biocompatible, inexpensive, superparamagnetic and has good electrochemical properties [4]. However, Fe_3O_4 has some disadvantages such as relatively low conductivity, low electron transfer rates and the possibility of self-agglomeration which results in the loss of magnetism and stability [5]. To maximise the reactivity of the nanostructured Fe_3O_4, graphene has received good attention as an ideal support material. Graphene is a two-dimensional thick planar sheet of sp^2-bonded carbon atoms densely arranged in a honeycomb crystal lattice. These bond and electron configurations offer a high electrical conductivity of graphene which is suitable as electrochemical sensor. Its high surface area (2630 $m^2 g^{-1}$) also provides a larger platform for building nanocomposites [6]. Thus, by creating Fe_3O_4/graphene nanocomposite, the agglomeration of the Fe_3O_4 nanoparticles is reduced, conserving their unique properties.

To the best of our knowledge, there is no report which is based on Fe_3O_4/graphene nanocomposite-modified electrode in the non-enzymatic glucose sensing application. Most of the previous studies still required glucose oxidase enzyme to detect the glucose. Based on these gaps in the literature, we have focused on the fabrication of the non-enzymatic glucose sensor based on Fe_3O_4/graphene nanocomposites. The nanocomposite was first synthesised by facile one-pot synthesis at a low temperature and short reaction time. Sodium carbonate was used as reducing agent and stabiliser. This synthesis method requires no toxic solvent and therefore it is environmental-friendly and can be simply controlled by changing the process parameters. Besides, via one-pot deposition reaction, the possibility of contamination resulting from Fe_3O_4/graphene nanocomposites was reduced. The analytical performance of the as-prepared Fe_3O_4/graphene-modified glassy carbon electrode (Fe_3O_4/graphene/GCE) was then investigated by characterising the sensitivity, limit of detection (LOD), linearity range, selectivity, reproducibility, and sensor stability.

2. EXPERIMENTAL

2.1. Reagents and materials

Graphite powder (spectral requirement, Merck Sdn. Bhd) was used for synthesising graphene oxide (GO) and graphene. Na_2CO_3, $NaNO_3$, KNO_3, LiCl, $FeSO_4.7H_2O$, NaOH, KH_2PO_4, K_2HPO_4,

D(+)-glucose, sucrose, D(-)-fructose, lactose monohydrate, sodium citrate dehydrate, DMF and NH_4OH solution were purchased from Merck Sdn. Bhd (Malaysia). All of these reagents were of analytical grade and used as received.

2.2. Apparatus

TEM measurement has been performed using transmission electron microscopy (TEM: JEOL-2000EX) to study the details morphology of Fe_3O_4/graphene nanocomposites The crystallinity and phase purity of the as-prepared Fe_3O_4 /graphene nanocomposites were examined by powder X-ray diffraction (XRD) patterns from a diffractometer of Bruker AXS (XRD: D8 Advance) with Cuκα radiation (λ = 1.54 Å). Raman spectra of Fe_3O_4/graphene nanocomposites were collected on a Renishaw InVia Raman spectroscopy using 514 nm Argon laser as the excitation source. The excitation power was set up in between 0.3 and 0.7 mW to limit heating of the samples. Fourier transform infrared (FTIR) spectroscopy was carried out on FTIR (Thermo Nicolet Nexus) using the KBr disc method. Electrochemical analysis was performed with a three-electrode system using Gamry Potentiostat Series-G750 (USA), consisting of a working electrode (bare or modified glassy carbon electrode), a reference electrode (an Ag/AgCl), and a counter electrode (platinum wire). The supporting electrolyte that has been used in this electrochemical measurements was 0.1 M KNO_3 solution.

2.3. Synthesis of Fe_3O_4/graphene nanocomposites

The typical synthesis of Fe_3O_4/graphene nanocomposites is as follows: approximately 30 mg of graphene oxide (GO) was dispersed in 20 mL deionised water via ultrasonication. $FeSO_4.7H_2O$ was added to this dispersion under stirring. Then, a drop wise addition of ammonia solution was added to adjust the pH value of the mixture. The pH value of the mixture was controlled at approximately 10 to 11. The mixture was continuing stirred for another 20 minutes. All the syntheses were completed under oxygen-free conditions to prevent the formation of maghemite, γ-Fe_2O_3, and hematite, α-Fe_2O_3. Finally, 1.0 M Na_2CO_3 solution was added to the solution and hydrothermal treatment was conducted for 3 hours at 100ºC ± 2ºC. The solution was then centrifuged and washed with de-ionised water and ethanol, and dried at 60ºC in the oven for 24 hours in order to collect the product. The final product was named as Fe_3O_4/graphene nanocomposites. In the absence of GO, the Fe_3O_4 nanoparticles were obtained via the same process. Similarly, graphene was prepared using our previous reported method without the presence of $FeSO_4$ [7].

2.4. Electrode preparation and electrochemical measurements

For each series of experiment, a 2.0 µL of Fe_3O_4/graphene nanocomposites suspension (1.0 mg/mL in DMF/water solution) was injected onto the surface of GCE and dried at room temperature. The resulting Fe_3O_4/graphene/GCE was then kept in a desiccator prior to further experiments. The

Fe_3O_4/graphene/GCE was evaluated as a glucose sensor in 0.1 M KNO_3 supporting electrolyte. Cyclic voltammetry (CV) measurements were studied in the potential range of +0.3 to +1.3 V. The steady state current response (chronoamperometry) was obtained at a constant potential of +0.6 V with reference to pseudo reference electrode Ag/AgCl. Electrochemical impedance spectroscopic (EIS) analysis was carried out in a 0.1 M KNO_3 solution at its open circuit potentials, in the frequency range of 0.01 to 100 kHz with a potential amplitude of 50 mV.

2.5. Determination of glucose in blood sample

The actual application of the Fe_3O_4/graphene/GCE was confirmed by glucose concentration detection in human blood serum samples. We have obtained the real human blood samples from the school hospital (Universiti Pendidikan Sultan Idris, Perak, Malaysia). The procedure was as follows: Firstly, the plasma was collected by centrifuging the obtained blood samples (2000 rpm for 5 minutes). Then, the collected plasma was aliquoted and stored at -20 $^{\circ}$C until analysis. For analysis step, the blood serum samples were diluted for 100 times using 0.1 M KNO_3 solution. Then, about 50 µL of diluted serum samples were added into 15 mL 0.1 M KNO_3 solutions and each sample was observed under optimised conditions as mean from three determinations. The current responses at +0.60 V were recorded between the as-prepared sensor and data provided using a clinical-used glucometer (Optimum Xceed). The comparison of *t*-test analysis were carried out for validation step. The recovery test was performed to study the practicability of the proposed method towards real sample analysis

3. RESULTS AND DISCUSSION

3.1. Characterisation of nanocomposites

The GO prepared by the modified Hummers method contained a lot of oxygenated functional groups (epoxy, hydroxyl-, carboxyl-) distributed on its surface [7]. These oxygenated functional groups act as a nucleation centre for the growth of Fe_3O_4 through electrostatic attraction of the ions. A TEM measurement has been performed to study the detailed morphology and structure of the Fe_3O_4/graphene nanocomposites. Fig. 1A provides the TEM image of the Fe_3O_4/graphene nanocomposites. It shows that the surface of the graphene sheet was densely covered with distributed Fe_3O_4 nanoparticles. The Fe_3O_4 nanoparticles have a narrow size distribution mainly in the range of 20 – 30 nm, as demonstrated by the corresponding size distribution histogram (inset Fig. 1A).

The crystallinity and phase purity of the as-prepared products were examined by XRD. Fig. 1B shows the XRD patterns of the Fe_3O_4 and Fe_3O_4/graphene nanocomposites, respectively. The series of diffraction peaks at 2θ = 23.8°, 29.2°, 32.1°, 37.0°, 38.3°, 47.1°, 50.7°, 56.5°, 60.0°, 67.3°, and 76.0° was assigned to reflections from the (120), (220), (311), (222), (400), (051), (422), (511), (440), (520) and (533) crystal plane of Fe_3O_4 (JCPDS no. 19-0629) [8]. The position of a broad peak at 24.8° (002) was an important peak of graphene [9]. Thus, the XRD observation confirmed the reduction of GO using Na_2CO_3 as a reductant and the successful deposition of Fe_3O_4 nanoparticles on the surfaces of

the graphene sheets by the one-pot chemical reduction reaction, which was consistent with the results of the TEM analysis.

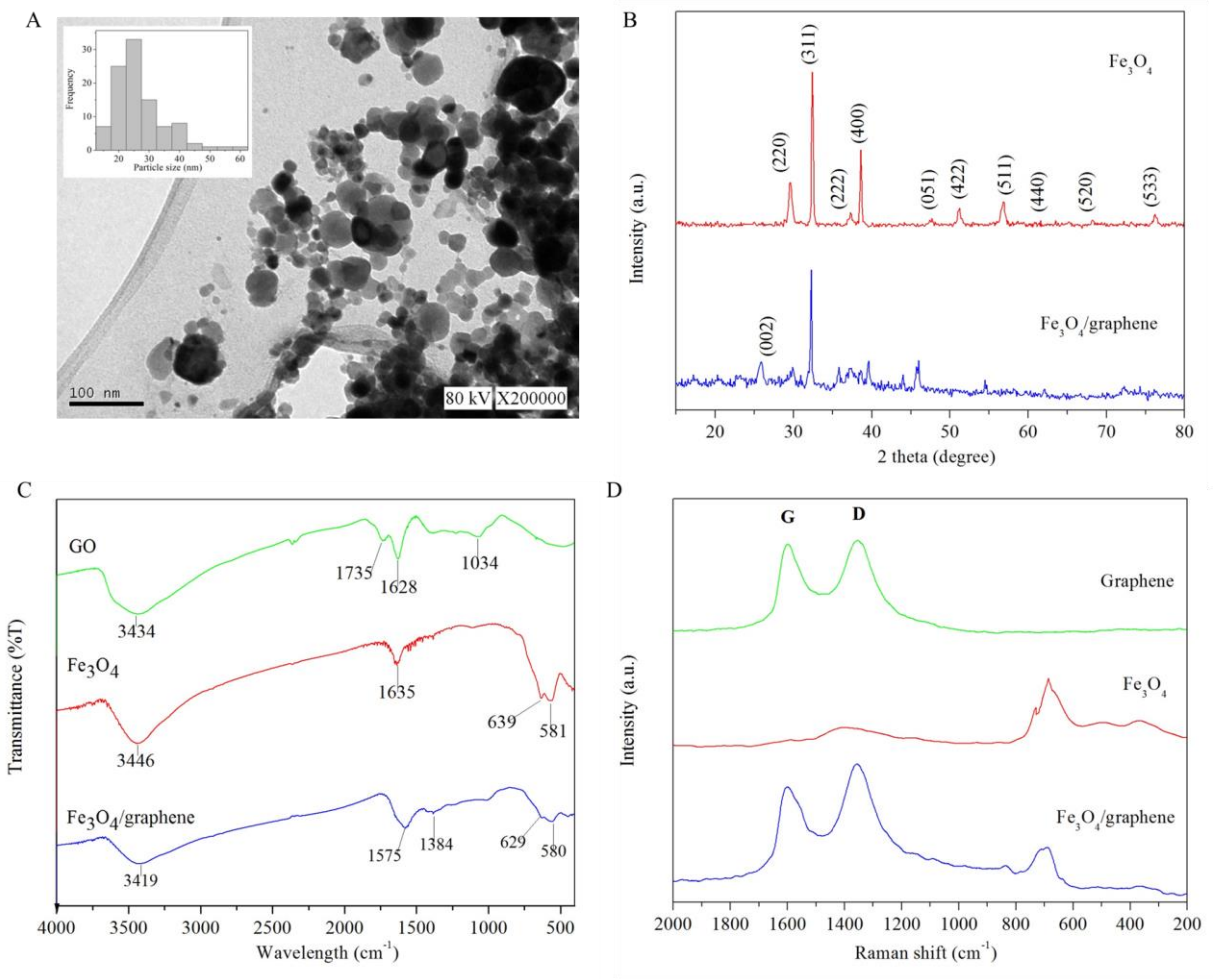

Figure 1. (A) TEM image of Fe_3O_4/graphene nanocomposites, (B) XRD patterns, (C) FTIR spectra, and (D) Raman spectra.

In Fig. 1C, the FTIR spectrum of GO presented O–H vibrations at 3434 cm^1, C=O stretching in carboxylic and/or carbonyl moiety bands at 1735 cm^{-1}, O–H bending and aromatic C=C, skeletal ring vibrations from the graphitic domain at 1628 cm^{-1}, O–H deformation in carboxylic moiety bands at 1384 cm^{-1}, and C–OH stretching in alcoholic moiety bands at 1065 cm^{-1} [10].The formation of graphene was further confirmed by reducing of the bands related with the oxygen-containing group and also the entirely varnishing of carboxyl C=O.peak at 1735 cm^{-1}. Meanwhile, the peaks at 629 cm^{-1} and 580 cm^{-1} were observed suggesting the presence of Fe_3O_4 nanoparticles and confirmed the formation of Fe_3O_4/graphene-nanocomposites [11].

The reduction of GO to form graphene in the composite material was also confirmed by the Raman analysis (Fig. 1D). The Raman spectrum of the Fe_3O_4/graphene nanocomposites shows two main characteristic bands of graphene at around 1369 and 1603 cm^{-1} which is consistent with the breathing mode of A_{1g} symmetry due to the phonon interaction near the K zone boundary (band D) and

the E_{2g} phonon mode of the sp^2 bonded carbon atoms (band G), respectively [12]. The D-band with higher intensity than G-band confirms the formation of graphene. The characteristic Raman scattering peak at 670 cm^{-1}, corresponding to the T_{2g} and A_{1g} vibration modes of Fe_3O_4, were observed for both Fe_3O_4 and Fe_3O_4/graphene nanocomposites [13].

3.2. Optimisation of sensor

Type of the supporting electrolyte was found to be crucially effective on the glucose sensor response which functions to reduce the resistance of the solution, thus producing an electrical signal proportional to the glucose. Fig. 2A presents the oxidation current responses of 0.1 mM glucose in NaOH, PBS, LiCl, NaCl, KNO_3, and $NaNO_3$, (each 0.1 M) that have been examined using CV. It is quite common in the literature review to discuss glucose oxidation using PBS and NaOH electrolytes. However, in this work, the oxidation of glucose at the as-prepared Fe_3O_4/graphene/GCE was not satisfactory by using these two common electrolytes in the system. With this, the voltammetric behaviour of Fe_3O_4/graphene/GCE towards glucose oxidation was further tested in supporting electrolyte containing 0.1 M solutions of alkali metal cations such as Li^+, Na^+, and K^+. It was found that the oxidation peak current is highest in the KNO_3 electrolyte, and the voltammogram shape was well defined. The oxidative peaks observed with the Fe_3O_4/graphene/GCE in the electrolyte solution containing the alkali cations increased with the increase of the ionic radius ($Li^+ < Na^+ < K^+$), demonstrating that the counter-ions affect the voltammetric behaviour of the electrode. Thus, the KNO_3 solution was chosen as the supporting electrolytes in the whole experiment for Fe_3O_4/graphene/GCE towards glucose sensing.

The effect of pH on the electrochemical reaction of glucose was investigated by varying the pH of the KNO_3 solution from pH 2.5 to 8 (Fig. 2B). The peak current increased with the increased of pH from 2.5 to 3 and reached its maximum at pH 3. The peak current gradually decreased as the pH increased from 4 to 8. This indicates that, at a low pH value, deprotonation process involve during the oxidation process of glucose on Fe_3O_4/graphene/GCE happen effectively. In contrast, at high pH solution, the electrocatalytic reaction was hard due to the shortage of proton [14].

When using supporting electrolytes, not only their pH, but the concentration is also taken into consideration. The CV of different concentrations of KNO_3 solutions were observed at 100 mV s^{-1} and showed that the voltammogram consists of one cathodic and one anodic peak in 0.1 mM glucose concentrations (Fig. 2C). Both the cathodic and anodic peak currents linearly increased with the increasing concentration of KNO_3 from 10 to 100 mM, and started to decrease with further increase in glucose concentration. This behaviour may be due to the presence of a large amount of electroactive species at higher concentration, disrupts the adsorption of glucose at the surface electrode.

To evaluate the kinetics of the glucose oxidation on the Fe_3O_4/graphene/GCE, the CV curves of the electrode in a 0.1 M KNO_3 solution containing 0.1 mM glucose at different scan rates were recorded (Fig. 2D). This result shows the quasi-reversible character of the electrode reaction, as the peak potential affected by the scan rate and peak current ratio (i_{pa}/i_{pc}) is not in unity [15].

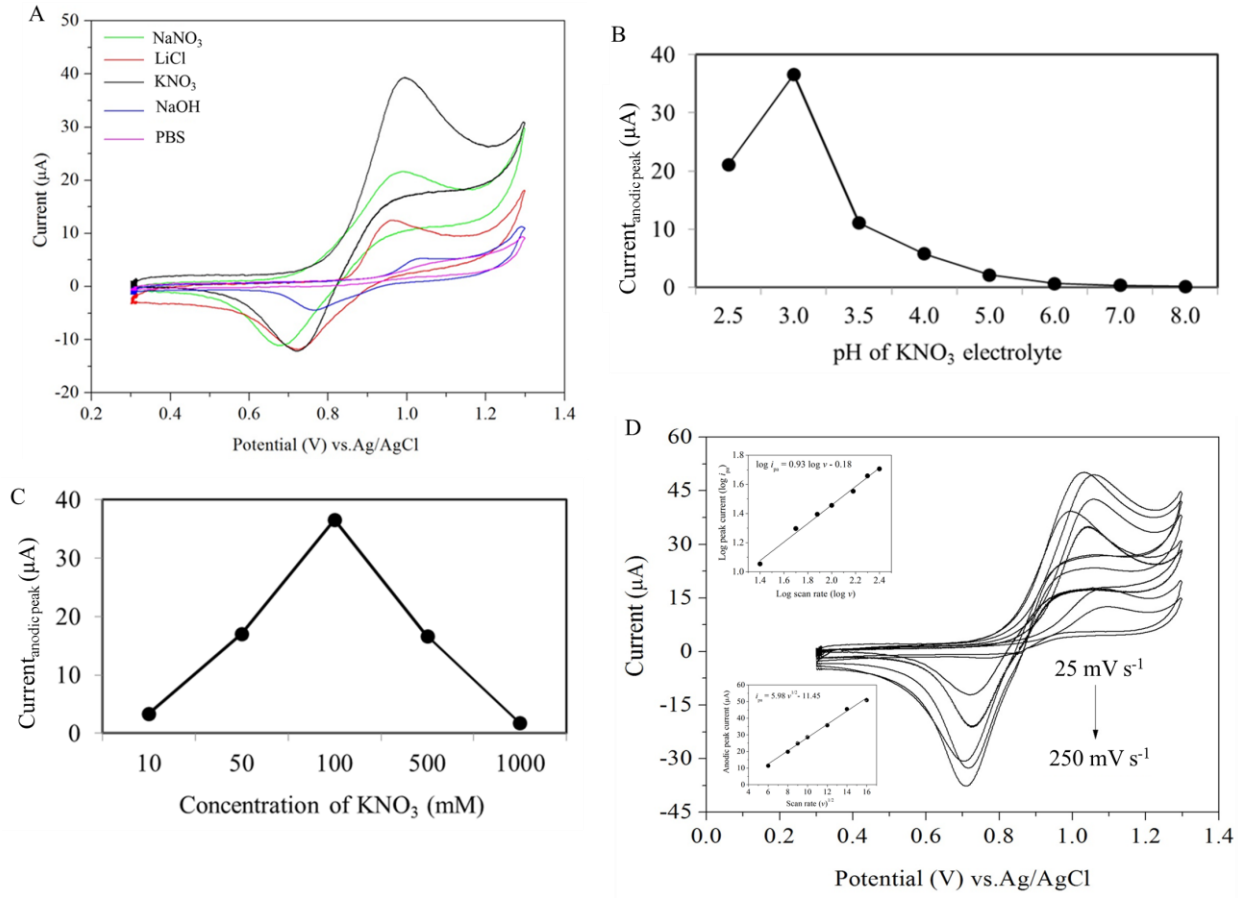

Figure 2. Effect of (A) types of electrolyte, (B) pH of electrolyte, (C) concentration of supporting electrolyte, and (D) scan rate towards glucose detection using Fe_3O_4/graphene/GCE sensor.

The equation related to the plot of the logarithm of peak current versus logarithm of scan rate was found to be $\log i_{pa} = 0.93 \log v - 0.18$ with coefficient of 0.990. The slope of this curve (0.93 $\log i_p/\log v$) is very close to the theoretical value of 1.0 for adsorption controlled processes [15,16]. A linear dependence of anodic peak intensity upon the square root of scan rates was found as the given equation $i_{pa} = 5.98\ v^{1/2} - 11.45$, which confirmed an adsorption behaviour.

3.3. Electrochemical behaviour of modified electrodes

The electrochemical performances of different modified electrodes to 0.1 mM glucose were measured by CV in 0.1 M KNO_3 at a scan rate of 100 mV s^{-1} (Fig. 3A). In the absence of glucose (see the inset of Fig. 3A), no redox peaks appeared at bare GCE, graphene/GCE, Fe_3O_4/GCE, and Fe_3O_4/graphene/GCE, respectively. After the addition of glucose, there were still no obvious glucose oxidation peaks for both bare GCE, and graphene/GCE, respectively. However, the background current was larger at the Fe_3O_4/GCE, representing the important role of Fe_3O_4 nanoparticles as electrocatalyts in glucose oxidation. Meanwhile, an obvious oxidation peak was observed at the Fe_3O_4/graphene/GCE, indicating that the nanocomposites has allowed glucose oxidation directly on the GCE without the use of enzymes. With addition of graphene, the current response of the modified

electrode was increased towards glucose, which may be due to the synergistic effect of both Fe_3O_4 nanoparticles and graphene, as well as to the enhanced conductivity and active surface area of the modified electrode [5].

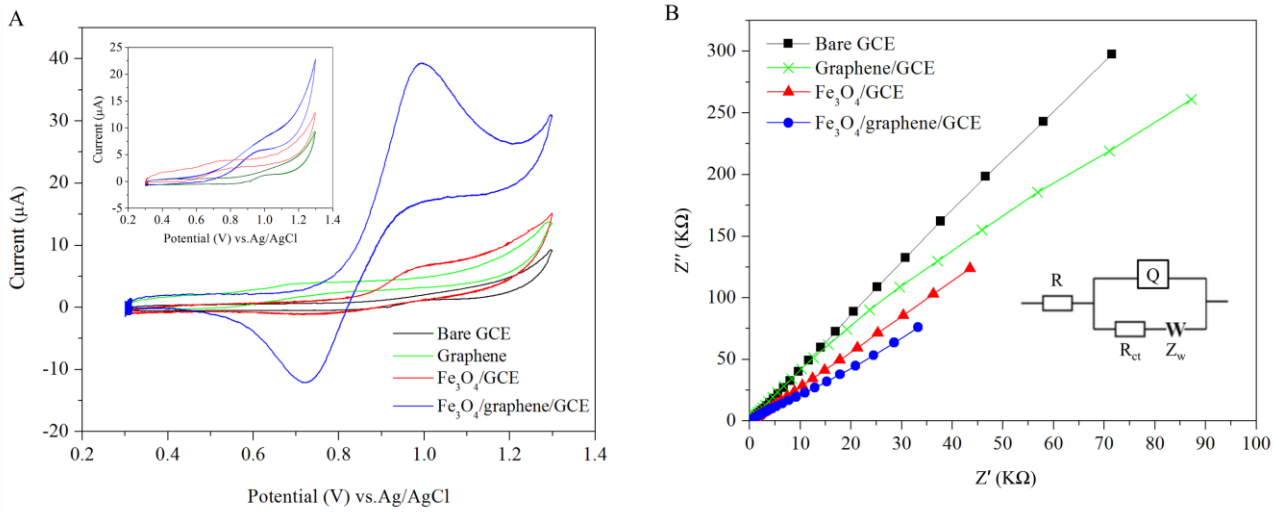

Figure 3. (A) CV curves in absence and presence of glucose, and (B) Nyquist plots of bare electrode and modified electrodes.

The integration of the nanostructured Fe_3O_4 in the electrode for this electrochemical circuit demonstrates high surface reaction and catalytic activity, large surface-to-volume ratio and strong adsorption ability that are beneficial in the detection of glucose. Moreover, the magnetic nature of Fe_3O_4 nanoparticles enables the formation of nanoparticle conductive on the electrode surface and simplifies the assembly of nanoparticles onto the electrode. Thus, Fe_3O_4/graphene nanocomposites are good in the fabrication of electrode assemblies since the magnetic field reinforces the attraction of the particles to the electrode's surface [17]. The electrochemical process may be suggested as follows [18].

$$2Fe(III) + glucose \rightarrow 2Fe(II) + gluconolactone + H_2O_2 \quad \text{(Eq. 1)}$$

$$gluconolactone + H_2O \rightarrow 2H^+ + gluconic\ acid \quad \text{(Eq. 2)}$$

$$2Fe(II) \rightarrow 2Fe(III) + 2e^- \quad \text{(Eq. 3)}$$

Electrochemical impedance was studied to reveal the impedance changes of the electrode surface. Fig. 3B shows the EIS of different electrodes, namely the bare GCE, graphene/GCE, Fe_3O_4/GCE and Fe_3O_4/graphene/GCE, respectively. The EIS analysis of these electrodes was performed with a frequency range of 0.01 to 100 kHz using 0.1 M KNO_3 as the supporting electrolyte. The low charge transfer resistance and good conductivity of the redox probe was presented by the almost straight line plots [19]. The Randles equivalent circuit (see the inset of Fig. 2B) includes the resistance of the electrolyte solution (R), the value of constant phase element (Q), the charge-transfer resistance (R_{ct}) and the wardburg impedance (Z_w). From the Nyquist plot, the R_{ct} value obtained were 13.67 Ω, 9.215 Ω, 5.759 Ω, and 1.576 Ω for the bare GCE, graphene/GCE, Fe_3O_4/GCE, and

Fe_3O_4/graphene/GCE, respectively. These results indicate that the electron transfer resistance is as follows: bare GCE > graphene > Fe_3O_4 > Fe_3O_4/graphene and the electron transfer ability were Fe_3O_4/graphene > Fe_3O_4 > graphene > bare GCE. This proved that after GO was reduced and Fe_3O_4 nanoparticles were deposited on the graphene sheets, the obtained Fe_3O_4/graphene nanocomposites had higher electric conductivity and improved the electron-transfer rate.

3.4. Amperometric performance towards glucose

Determination of glucose on the Fe_3O_4/graphene/GCE was conducted by the amperometric method. The effect of applied potential on the sensor response was studied and the results are shown in Fig. 4A. The current response towards glucose increased with the change of applied potential from +0.3 V to +0.7 V. The highest sensitivity was obtained at +0.6 V with a fast response time (less than 3 seconds) of the modified electrode when adding glucose into the KNO_3 supporting electrolyte. A further increase of the current potential resulted in the decrease of current response. Therefore, +0.6 V was selected as the applied potential in the amperometric detection of glucose. The calibration curve of the Fe_3O_4/graphene/GCE to the different concentrations of glucose obtained in N_2-saturated KNO_3 0.1 M (pH = 3) is shown in Fig. 4B. The calibration curve presented a linear relationship towards glucose from 50 µM to 4.00 mM.

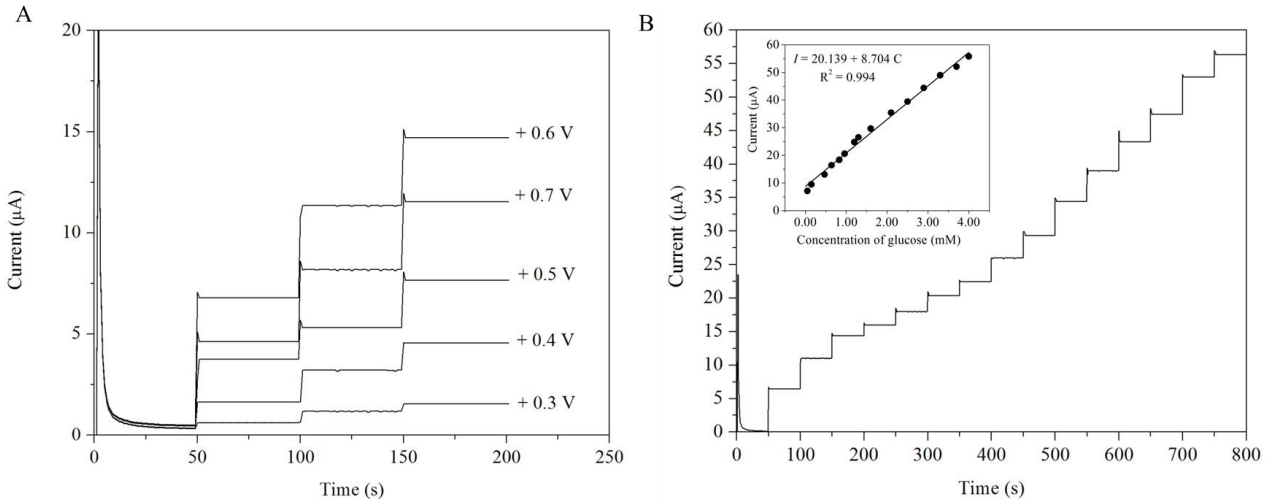

Figure 4. (A) Amperometric responses of Fe_3O_4/graphene/GCE at different potentials, and (B) amperometric responses at +0.60 V with addition of certain concentration of glucose.

The linear equation was given by I = 20.l39 + 8.704 C, where I and C represent the response current (µA) and glucose concentration (µM), respectively (R^2 = 0.994). The sensitivity of the sensor with surface area of 0.021 cm^2 was found to be 959.00 µA mM^{-1} cm^{-2} and the limit of detection (LOD) was calculated to be 0.18 µM. The comparison of the analytical performances of Fe_3O_4/graphene/GCE with previous studies is summarized in Table 1.

Table 1. Performance of Fe_3O_4/graphene nanocomposites glucose sensor compared with other reported.

Modified electrode	Types of electrochemical sensor	Sensitivity ($\mu A\ mM^{-1}\ cm^2$)	Linear range (mM)	LOD (μM)	Reference
Fe_3O_4/silica/Au	Enzymatic	62.45	up to 3.97	0.23	[20]
Fe_3O_4/graphene/GCE	Enzymatic	-	0.5 to 12	5000.00	[21]
Fe_3O_4/graphene/ magnetic GCE	Enzymatic	5.32	0.05 to 1.5	0.15	[22]
Fe_3O_4 chitosan/graphene	Enzymatic	5.658×10^3	up to 26	16.00	[23]
Graphene wrapped Cu_2O nanocubes	Non-enzymatic	285.00	0.3 to 3.3	3.3	[25]
Au@Cu_2O/Nafion/GCE	Non-enzymatic	715.00	0.05 to 2.00		[26]
Nafion/Graphene/Co_3O_4	Non-enzymatic	560.00	-	0.30	[27]
NiO quantum dots modified ZnO nanorods	Non-enzymatic	13.14 and 7.31	0.001 to10.00 and 10 to 50	-	[28]
Fe_3O_4/graphene/GCE	Non-enzymatic	959.00	0.05 to 4.00	0.18	This work

3.5. Selectivity, reproducibility, and stability

The interference from electroactive compounds normally existing with glucose in human blood sample such as ascorbic acid (AA), dopamine (DA), uric acid (UA), sucrose (suc), lactose (lac), fructose (fruc), NaCl and sodium citrate (cit), may cause accuracy problems in the determination of glucose. In human blood, those of the commonly interfering species was 30 times lower than the concentration of glucose [24]. According to this, the interferences study was carried out by measuring the amperometric response to successive addition of 0.1 mM glucose and 0.05 mM of interfering species in 0.1 M in KNO_3 supporting electrolyte. Based on Fig. 5A, the results indicated that these interfering species did not cause an obvious interference for glucose sensing, demonstrating a good selectivity of Fe_3O_4/graphene/GCE as a glucose sensor.

In addition, the interference tests of the sensor were also examined in 0.1 M KNO_3 solution with successive addition of 0.01 mM NaCl at the applied potential of +0.6 V vs. Ag/AgCl. This is because the poisoning effect from chloride ions can interrupt the activities of most of the non-enzymatic glucose sensors based on precious metals or alloys. From Fig. 5A, it was found that the current response of glucose oxidation was not interrupted by the addition of chloride ions. Moreover, a negligible effect was also presented by the addition of sodium citrate. This indicates that the as-prepared Fe_3O_4/graphene/GCE has a very good selectivity and makes this sensor as a promising candidate for glucose sensing application.

The reproducibility of the developed sensor were further studied (Fig. 5B). The relative standard deviation (RSD) with five different sensors prepared under the same conditions was 2.81 %, showing that the sensor was stable and could be used repeatedly for the detection of glucose without poisoning by the oxidation products.

The stability of the sensor was evaluated by measuring the current response to glucose within 14 days. The results presented that the current retains over 91% of its initial response after two weeks of storage, indicating the long term stability of Fe_3O_4/graphene/GCE. The amperometric response current of the Fe_3O_4/graphene/GCE decreased to less than 5% after 2000 seconds continuous measurement (see the inset of Fig. 5B). These results suggested that the sensor has long term stability for glucose detection.

The *t*-test was carried out for validation step. The values obtained between Fe_3O_4/graphene/GCE sensor and data provided using a clinical-used glucometer (Optimum Xceed) were monitored as mean from three determinations. From findings, the values achieved by our sensor were consistent with those measured by a clinical-used glucometer (Optimum Xceed) (Table 2). There was no difference between the data obtained using the two methods at the 95% confidence level.

Table 2. Validation test for detection of glucose (n = 3).

Sample	Proposed method (mM)	Glucometer (mM)	*t*-value	critical *t*-value	*p*-value
1	1.57 ± 0.21	1.6 ± 0.2	0.18	2.13	0.43
2	2.24 ± 0.26	2.3 ± 0.1	0.31	2.35	0.37
3	3.48 ± 0.23	3.6 ± 0.2	0.59	2.24	0.26

A

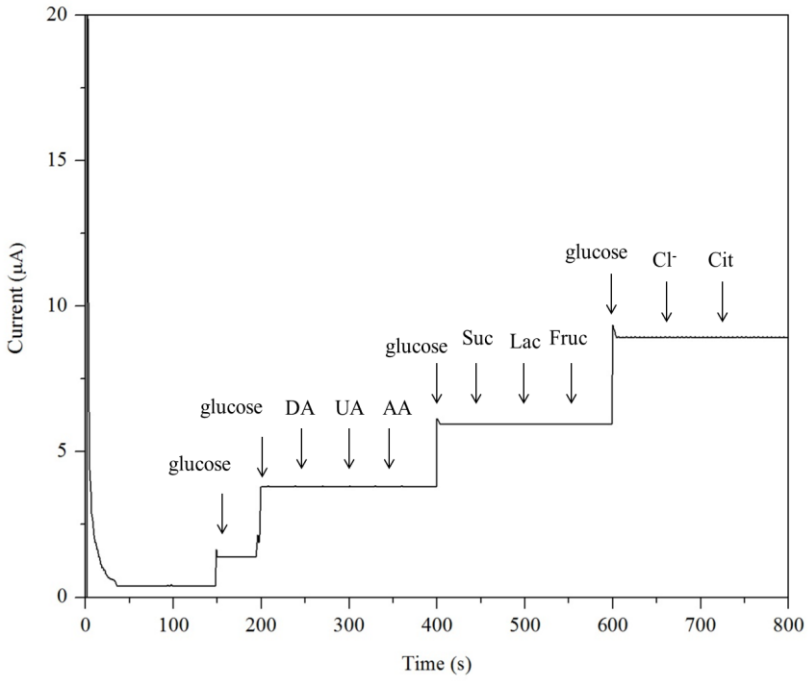

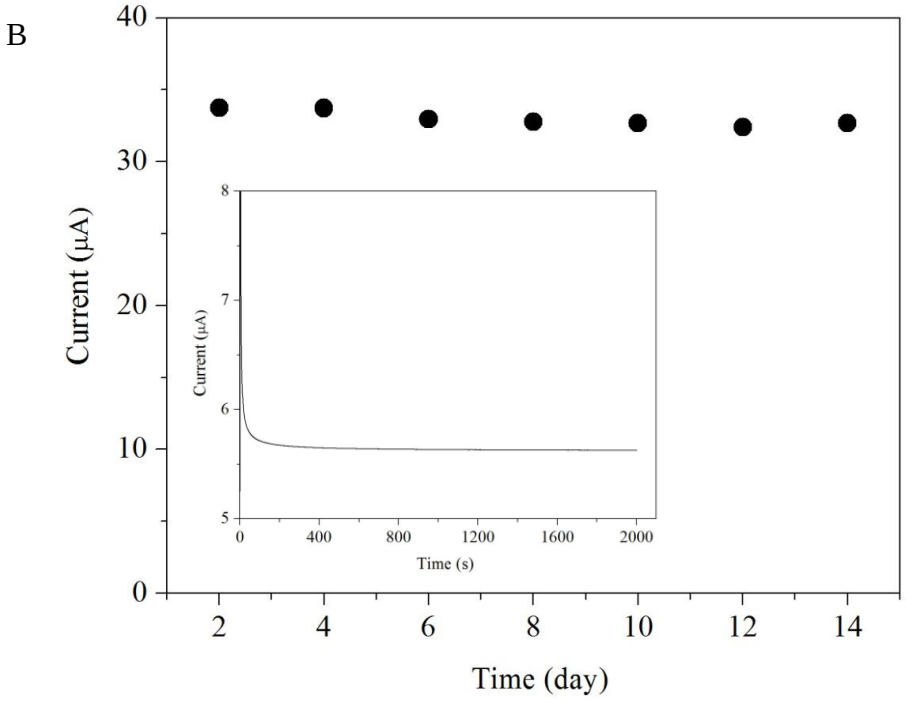

Figure 5. (A) Interference measurements in the presence of glucose (0.1 mM) and addition of 0.05 mM interferents species, and (B) stability test of Fe_3O_4/graphene/GCE.

3.6. Real samples analysis

For real sample analysis, the proposed method was conducted for detecting the glucose in human blood serum. Firstly, about 50 µL of diluted blood serum samples were added into 15 mL KNO_3 solution (0.1 M). Each sample was experimental under optimised conditions as mean from three determinations. Then, about 15 µL of 0.1 M pure glucose stock solution was introduced in the above solution, followed by the addition diluted glucose ranged from 1.40 mM to 3.09 mM. With concerning the previously calibration curve, the amount of glucose in the initial blood samples was then calculated. After the calculation, it was found that the obtained recoveries of the proposed method ranged from 98.59 to 101.64% suggesting good accuracy of the method (Table 3). As conclusion, based on the recovery study and the comparison with a clinical-used glucometer, the proposed method explains the potential application of the proposed method for detecting glucose in biological samples.

Table 3. Recovery analysis of glucose in human blood serum samples (n = 3).

Sample	Detected (mM)	Added (mM)	Found (mM)	Recovery (%)
1	0.42	1.00	1.40	98.59
2	1.25	1.00	2.23	99.11
3	2.04	1.00	3.09	101.64

4. CONCLUSIONS

Fe_3O_4/graphene nanocomposites have been synthesized via green and simple one pot synthesis of the chemical reduction method in the alkaline aqueous system. High sensitivity, very selective towards glucose, good reproducibility and long term stability of Fe_3O_4/graphene/GCE were shown in the amperometric current-time measurements and could be considered as a promising electrode material for glucose sensing applications.

ACKNOWLEDGEMENTS
This publication is a part of the collaboration research between UNY and UPSI. We would like to deliver our gratitude to the Rector of UNY who support this research. We also thank to FMIPA Dean and Head of BBTKL that give license of Laboratory and instrument to running this research. The authors are also gratefully acknowledge the financial supports by Ministry of Higher Education Malaysia through Exploratory Collaboration Research Grant Scheme (ERGS) grant number: 2013-0082-102-22.

References

1. J.Wang, *Chem. Rev*., 108 (2008) 814.
2. R.Wilson and A.P.F.Turner, *Biosens. Bioelectron.*, 7 (1992) 165.
3. S.N.A.M.Yazid, I.M.Isa, S.A.Bakar, N.Hashim, and S.A.Ghani, *Anal. Lett.*, 47 (2014) 1821.
4. 4. L.L.Cao, S.M.Yin, Y.B.Liang, J.M.Zhu, C.Fang, and Z.C.Chen, *Mater. Res. Innov*., 19 (2015) S1.
5. Y.Liu, L.Zhou, Y.Hu, C.Guo, H.Qian, F.Zhang, and X.W.D.Lou, *J. Mater. Chem*., 21 (2011) 18359.
6. A.K.Geim and K.S.Novoselov, *Nat. Mater*., 6 (2007) 183.
7. S.N.A.M.Yazid, I.M.Isa, S.A.Bakar, and N.Hashim, *Int. J. Electrochem. Sci.*, 10 (2015) 7977.
8. P.S.Teo, L.N.Lim, M.N.Huang, C.H.Chia, and I.Harrison, *Ceram. Int*., 38 (2012) 6411.
9. Y.Jin, S.Huang, M.Zhang, M.Jia, and D.Hu, *Appl. Surf. Sci.*, 268 (2013) 541.
10. S.Park, J.An, R.Piner, I.Jung, D.Yang, A.Velamakanni, S.T.Nguyen, and R.S.Ruoff, *Chem. Mater*., 20 (2009) 6592.
11. Y.Wei, B.Han, X.Hu, Y.Lin, X.Wang, and X.Deng, *Procedia. Eng.*, 27 (2012) 632.
12. M.S.Dresselhaus, G.Dresselhaus, M.A.Pimenta, and L.M.Malard, *Phys. Rep.*, 473 (2009) 51.
13. H.Li, L.Qin, Y.Feng, L.Hu, and C.Zhou, *J. Magn. Magn. Mater.*, 384 (2015) 213.
14. K.S.Ngai, W.T.Tan, Z.Zainal, R.M.Zawawi, and M.Zidan, *Int. J. Electrochem. Sci.*, 8 (2013) 10557.
15. R.Holz, *Ber. Bunsen. Phys.*, 98 (1994) 1350.
16. İ.H.Taşdemir, M.A.Akay N.Erk, and E.Kılıç, *Electroanal.*, 22 (2010) 2101.
17. K.J.Cash and H.A.Clark, *Trends. Mol. Med.* 16 (2010) 584.
18. C.Xia and W.Ning, *Electrochem. Commun.*, 12 (2010) 1581.
19. H.Fan, Y.Li, D.Wu, H.Ma, K.Mao, D.Fan, B.Du, H.Li, and Q.We, *Anal. Chim. Acta*, 711 (2012) 24.
20. A.J.Wang, Y.F.Li, Z.H.Li, J.J.Feng, Y.L.Sun, and J.R.Chen, *Mater. Sci. Eng.* C, 32 (2012) 1640.
21. H.Teymourian, A.Salimi, and S.Firoozi, *Electroanal.*, 26 (2014) 129.
22. Y.Yu, H.Wu, B.Wu, Z.Wang, H.Cao, C.Fu, and N.Jia, *Micro. Nano. Lett.*, 6 (2014) 258.
23. W.Zhang, X.Li, R.Zou, H.Wu, H.Shi, S.Yu and Y.Liu, *Sci. Rep.*, 5 (2015) 11129.

24. J.Chen, W.D.Zhang and J.S.Ye, *Electrochem. Commun.*, 10 (2008) 1268.
25. M.Liu, R. Liu and Chen.W, *Biosens Bioelectron.*, 45 (2013) 206.
26. Y.Su, H.Guo, Z.Wang, Y.Long, W.Li, and Y.Tu, *Sens Actuators B Chem*., 255 (2018) 2510.
27. A.A. Ensafi, M.J. Asl, and B.Rezaei, *Talanta.*, 103 (2013), 322.
28. R.Ahmad, and Y.B. Hahn, *J Colloid Interface Sci.*, 512 (2018) 21.